# Dynamic percolation of spheres in a continuum: The case of microemulsions

C. Boned, J. Peyrelasse, and Z. Saidi
*Laboratoire de Physique des Matériaux Industriels, Université de Pau et des Pays de l'Adour, Centre Universitaire de Recherche Scientifique, Avenue de l'Université, 64000 Pau, France*
(Received 9 July 1992)

Results obtained on electrical conductivity, dielectric relaxation (static permittivity and characteristic frequency), and dynamic viscosity are presented for microemulsions with very different components (water-based or waterless, ternary or quaternary). However, they do have in common the fact that they all correspond to the model of a distribution of spheres, subjected to Brownian motion, dispersed in a continuous medium. For all these systems the associated dynamic percolation model is qualitatively verified. Moreover when the conditions of application of the asymptotic laws of the theory are satisfied, the scale exponents are the same (approximately equal to 2 above the threshold and $-1.2$ below it) for all the systems, in agreement with the theoretical predictions. This reflects the fact that all these systems belong to the same class of universality.

PACS number(s): 82.70.−y, 77.22.Gm, 66.20.+d, 05.40.+j

## I. INTRODUCTION

Over the past few years the phenomenon of percolation in microemulsions has been the subject of a large number of investigations. It was through the study of electrical conductivity $\sigma$ that it was first shown to exist [1] in water-in-oil microemulsions of the quaternary water–cyclohexane–1-pentanol–sodium dodecyl sulfate system. Subsequently, study into percolation concentrated above all on ternary systems involving the surfactant AOT [sodium bis(2-ethylhexyl) sulfosuccinate]. Occasionally glycerol was substituted for the water and in that case percolation can be clearly demonstrated [2] by studying the dynamic viscosity $\eta$. The reader will find a number of references in a recent article [3]. The different studies indicate that when microemulsions present the phenomenon of percolation (it should be recalled that not all microemulsions present this phenomenon) it seems to obey the dynamic model of percolation of spheres within a continuous medium, one of the characteristics of which is that the value of the percolation exponent below the threshold is $-1.2$ (whereas in the static case one obtains $-0.7$). References [4–8] give good evidence of this, but only for the electric conductivity and the dielectric relaxation and only in the particular case of the ternary system water-AOT-oil.

In this paper we will discuss results which clearly confirm the generality of the description. For ternary and quaternary systems of very different natures an identical description can be obtained if care is taken to limit the field of study to systems corresponding to the model of spheres in a continuous medium. For this reason we have studied systems which, in the light of the structural studies undertaken by other authors (often by neutron-scattering diffusion), seem likely to satisfy this description.

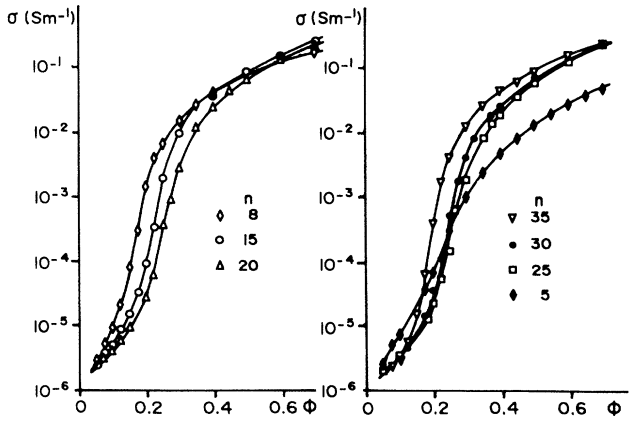


FIG. 1. Water-AOT-undecane system. $T=25$°C. Variations of $\log_{10}(\sigma)$ vs $\phi$ for different values of $n$ ($n$ is the molar ratio [water]/[AOT]).

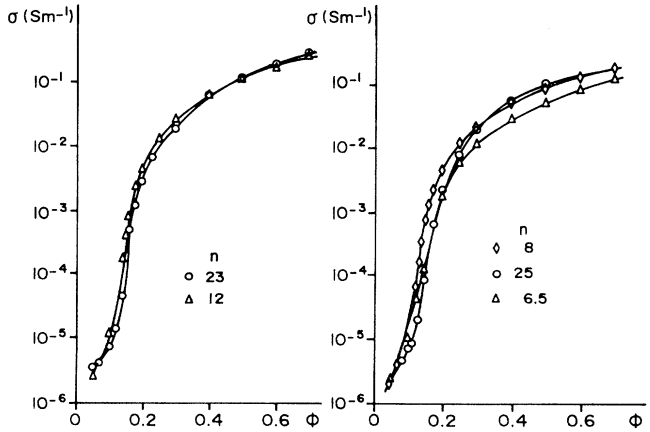


FIG. 2. Water-AOT-dodecane system. $T=25$°C. Variations of $\log_{10}(\sigma)$ vs $\phi$ for different values of $n$ ($n$ is the molar ratio [water]/[AOT]).

 

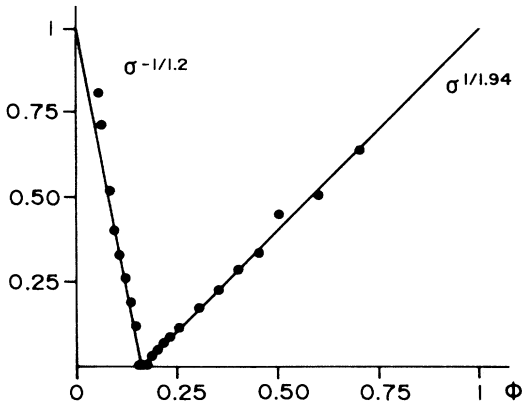


FIG. 3. Water-AOT-undecane system. $T=15°C$; $n=8$. Variations of $\sigma^{1/\mu}$ and $\sigma^{-1/s}$ vs $\phi$ (normalized to 1 for $\phi=0$ and 1). ●, experimental data; ——, theoretical curve [Eqs. (3) and (5)].

## II. EXPERIMENTAL TECHNIQUES

Electrical conductivity $\sigma$ is measured with a Wayne-Kerr B 331 precision bridge at 1592 Hz. The measurement cell is of the Philips-Mullard type and is calibrated using aqueous solutions of KCl. The relative uncertainty for $\sigma$ is estimated at 0.1%. Kinematic viscosity is measured with a Viscotimer Lauda S/1 capillary viscometer. Density is measured with an automatic Anton-Paar KG DMA 45 densitometer. Absolute uncertainty is less than $10^{-3}$ g/cm$^3$. Relative uncertainty for the dynamic viscosity $\eta$ is less than 0.5%. Finally the dielectric relaxation of these systems is measured using a Hewlett-Packard 4192-A impedance-meter controlled by a microcomputer. The measuring cell is a total influence Ferisol cell. For frequencies higher than 1 MHz we also used a time-domain dielectric spectroscopy system developed in the laboratory.

The substances used are distilled water, glycerol (Aldrich, purity > 99%), formamide (Sigma ACS reagent), ethylene glycol (Sigma), AOT (Sigma, purity > 99%), SDS (sodium dodecyl sulfate, Fluka, purity > 99%), isooctane (Fluka, purity > 99.5%), cyclohexane (Fluka, purity > 99%), undecane (Fluka, purity > 99%), dodecane (Fluka, purity > 98%), toluene (Fluka, purity > 99%), and 1-butanol (Fluka, purity > 99.5%). The samples are characterized by the volume fraction $\phi$ in dispersed matter.

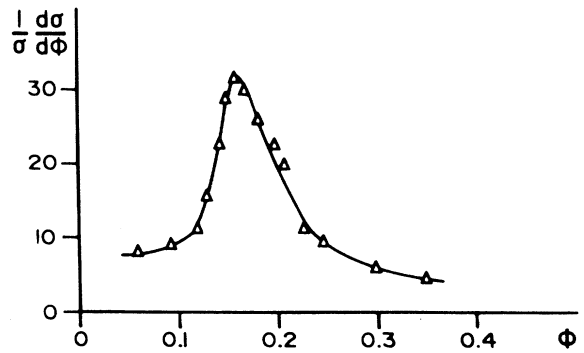


FIG. 4. Water-AOT-undecane system. $T=15°C$; $n=$[water]/[AOT]$=8$. Variations of $(1/\sigma)(d\sigma/d\phi)$ vs $\phi$.

## III. THEORETICAL MODELS

Analysis of the different investigations carried out on percolation show that the following relationships can be adopted as asymptotic behavior laws [3]. It is generally assumed that the system is made up of two components (1) and (2) and that $\phi$ is the volume fraction of component (1). The complex permittivity $\epsilon^*$ can be written

$$\frac{\epsilon^*}{\epsilon_1^*}=|\phi-\phi_c|^{\mu}f\left[\frac{\epsilon_2^*/\epsilon_1^*}{|\phi-\phi_c|^{(\mu+s)}}\right]=|\phi-\phi_c|^{\mu}f(z)\ , \qquad (1)$$

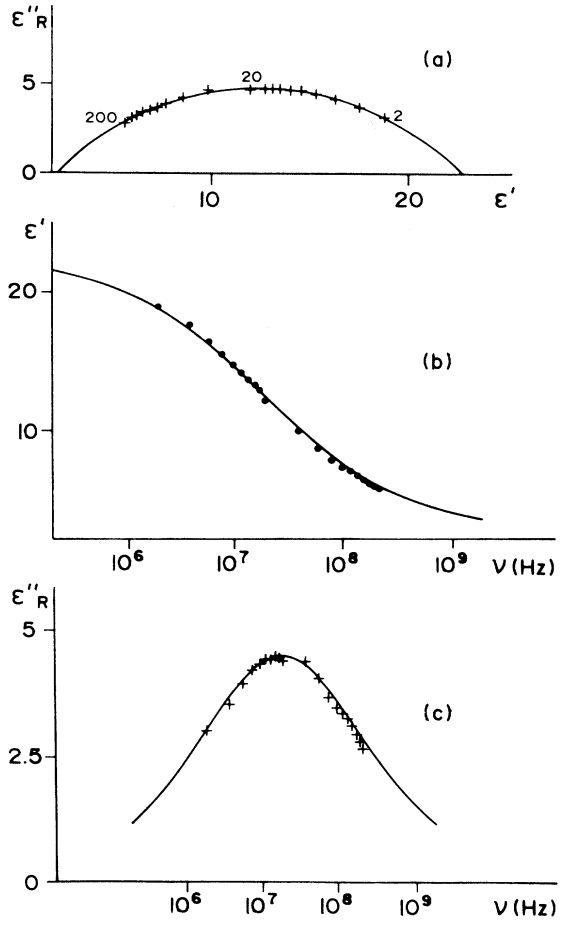


FIG. 5. Water-AOT-isooctane system. $T=25°C$; $n=$[water]/[AOT]$=8$; $\phi=0.30$. (a) $\epsilon_R''(\epsilon')$ curve. Frequencies are in MHz ($\nu_R=19$ MHz). (b) Variations of $\epsilon'$ vs frequency. (c) Variations of $\epsilon_R''$ vs frequency.

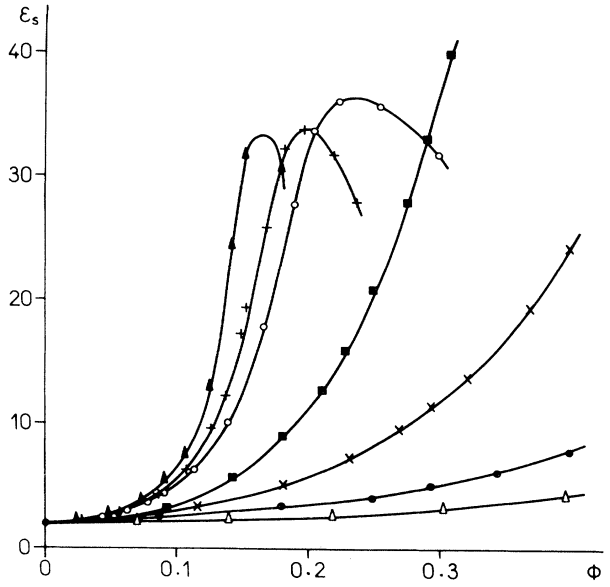


FIG. 6. Water-AOT-dodecane system. $T=25°C$. Variations of $\epsilon_s$ vs $\phi$ for different values of $n=$[water]/[AOT]. △, 0; ●, 2; $X=3.6$; ■, 4.4; ○, 6; +, 7; ▲, 10.

in which $\phi_c$ is the percolation threshold and $\mu$ and $s$ the characteristic exponents. The function $f(z)$ satisfies the following asymptotic forms:

$$f(z)=\begin{cases} C_1+C_1'z & \text{if } \phi>\phi_c+\delta_1,\ |z|\ll 1 \\ C_2 z & \text{if } \phi<\phi_c-\delta_2,\ |z|\ll 1 \end{cases}.$$

If it is assumed that the two components are conductors with conductivities $\sigma_1$ and $\sigma_2$ and the permittivities $\epsilon_{1s}$ and $\epsilon_{2s}$, one can write

$$\epsilon_1^*=\epsilon_{1s}-j\sigma_1/(2\pi\epsilon_0\nu)\ ,\quad \epsilon_2^*=\epsilon_{2s}-j\sigma_2/(2\pi\epsilon_0\nu)\ ,$$

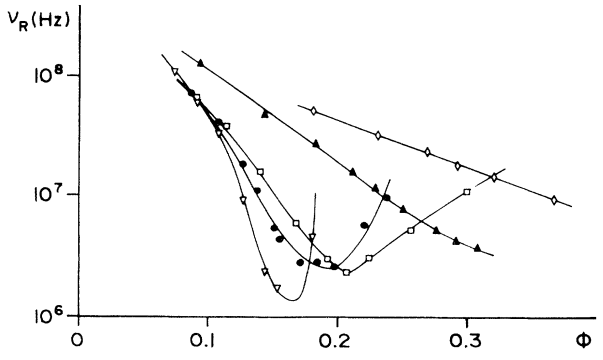


FIG. 7. Water-AOT-dodecane system. $T=25°C$. Variations of $\nu_R$ vs $\phi$ for different values of $n=$[water]/[AOT]. ◇, 3.6; ▲, 4.4; □, 6; ●, 7; ▽, 10.

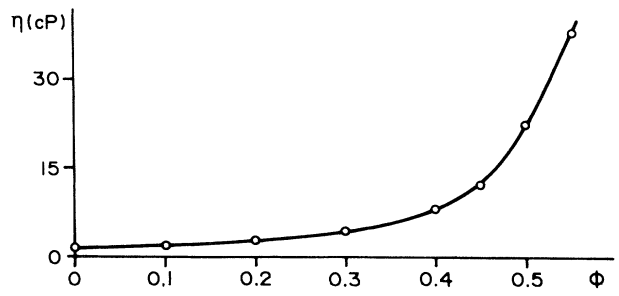


FIG. 8. Water-AOT-cyclohexane system. $T=25°C$; $n=$[water]/[AOT]$=13$. Variations of $\eta$ vs $\phi$.

in which $\epsilon_0$ is the dielectric permittivity of a vacuum, $\nu$ the frequency of the electric field applied, and $j^2=-1$. The system then presents the conductivity $\sigma$ and the dielectric constant $\epsilon_s$ such that

$$\left.\begin{aligned} \epsilon_s&=C_2\epsilon_{2s}(\phi_c-\phi)^{-s} \\ \sigma&=C_2\sigma_2(\phi_c-\phi)^{-s} \end{aligned}\right\} \text{ if } \phi<\phi_c-\delta_2,\ |z|\ll 1\ , \quad (2),\ (3)$$

$$\epsilon_s=C_1'\epsilon_{2s}(\phi-\phi_c)^{-s}+C_1\epsilon_{1s}(\phi-\phi_c)^{\mu}$$

$$\text{if } \phi>\phi_c+\delta_1,\ |z|\ll 1\ . \quad (4)$$

As the exponents $\mu$ and $s$ are positive, it can be seen that in the neighborhood of $\phi_c$, $\epsilon_s\alpha|\phi-\phi_c|^{-s}$ is obtained to either side of the percolation threshold. However, it

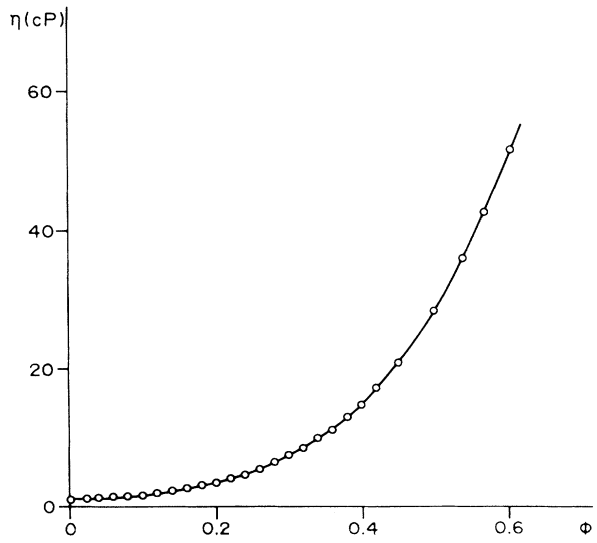


FIG. 9. Water-AOT-undecane system. $T=25°C$; $n=$[water]/[AOT]$=25$. Variations of $\eta$ vs $\phi$.

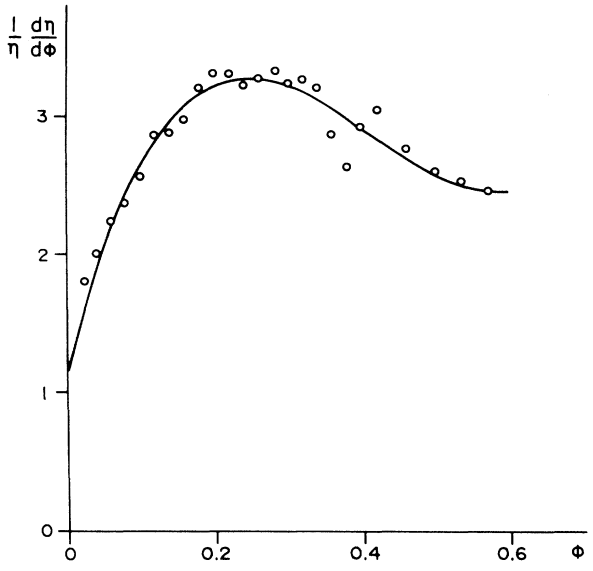


FIG. 10. Water-AOT-undecane system. $T=25°C$; $n$ = [water]/[AOT] = 25. Variations of $(1/\eta)(d\eta/d\phi)$ vs $\phi$.

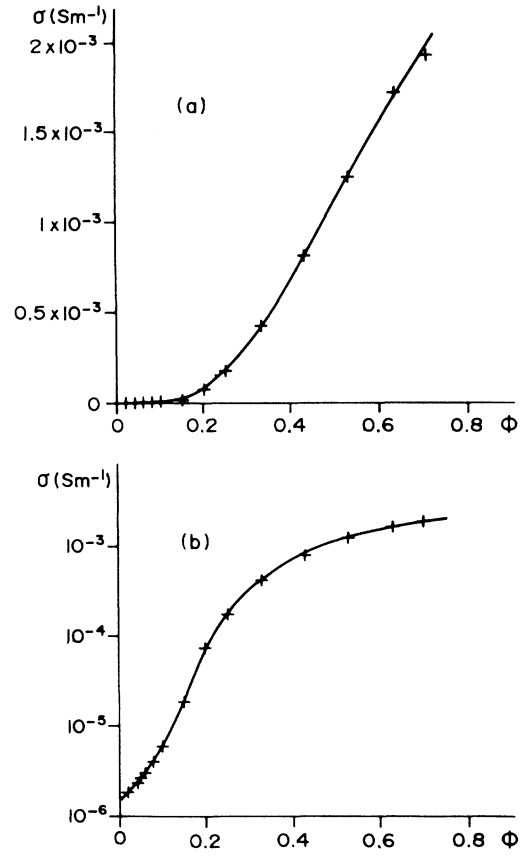


FIG. 11. Glycerol-AOT-isooctane system. $T=25°C$; $n$ = [glycerol]/[AOT] = 3.2. Variations of $\sigma$ vs $\phi$. (a) Curve $\sigma=f(\phi)$. (b) Curve $\log_{10}(\sigma)=f(\phi)$.

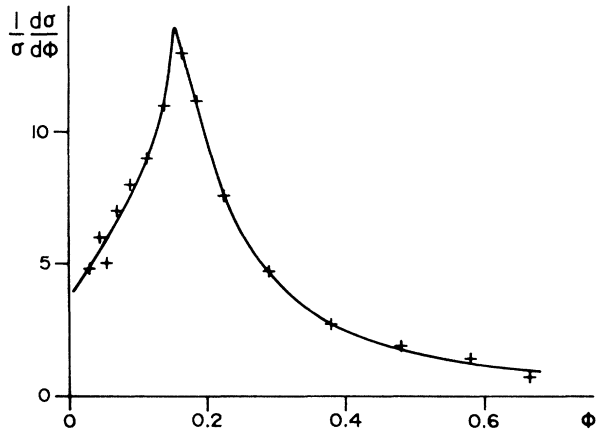


FIG. 12. Glycerol-AOT-isooctane system. $T=25°C$; $n$ = [glycerol]/[AOT] = 3.2. Variations of $(1/\sigma)(d\sigma/d\phi)$ vs $\phi$.

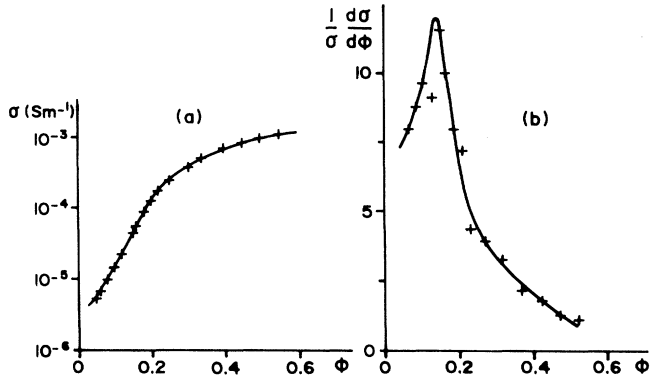


FIG. 13. Formamide-AOT-cyclohexane system. $T=25°C$; $n$ = [formamide]/[AOT] = 2.5. (a) Variations of $\log_{10}(\sigma)$ vs $\phi$. (b) Variations of $(1/\sigma)(d\sigma/d\phi)$ vs $\phi$.

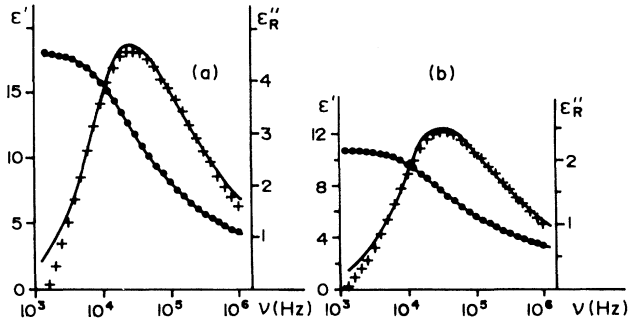


FIG. 14. Glycerol-AOT-isooctane system $n$ = [glycerol]/[AOT] = 4. Variations of $\epsilon'$(●) and $\epsilon''_R$ (+) vs frequency. (a) $T=10°C$; $\phi=0.20$. (b) $T=20°C$; $\phi=0.12$.

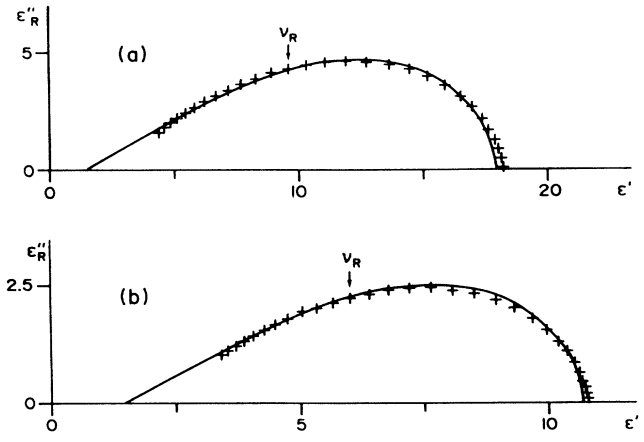


FIG. 15. Glycerol-AOT-isooctane system. $n$=[glycerol]/[AOT]=4. Variations of $\epsilon_R''$ vs $\epsilon'$. (a) $T$=10°C; $\phi$=0.20. (b) $T$=20°C; $\phi$=0.12.

should be pointed out that in Eq. (4) when $\phi$ moves away from $\phi_c$ (with $\phi > \phi_c$) the term $C_1'\epsilon_{2s}(\phi-\phi_c)^{-s}$ decreases and the term $C_1\epsilon_{1s}(\phi-\phi_c)^{\mu}$ increases . So depending on the values of $C_1$, $C_1'$, $\epsilon_{1s}$, and $\epsilon_{2s}$, the curve $\epsilon_s(\phi)$ may either present a clearly marked maximum, or a maximum followed by a more or less pronounced minimum. When increasing term is predominant, one might expect to observe experimentally a continuously increasing curve for $\epsilon_s(\phi)$

$$\sigma = C_1\sigma_1(\phi-\phi_c)^{\mu}\left[1+\frac{C_1'}{C_1}\frac{\sigma_2}{\sigma_1}(\phi-\phi_c)^{-(\mu+s)}\right]$$

$$\text{if } \phi > \phi_c+\delta_1,\ |z| \ll 1$$

and it will be observed that if $\sigma_2/\sigma_1 \ll 1$ (for example, for a perfect insulator $\sigma_2=0$), even very close to the threshold, the condition $\sigma_2/\sigma_1 \ll (\phi-\phi_c)^{(\mu+s)}$ is satisfied and one therefore obtains

$$\sigma = C_1\sigma_1(\phi-\phi_c)^{\mu} \text{ if } \phi > \phi_c+\delta_1,\ |z| \ll 1 . \tag{5}$$

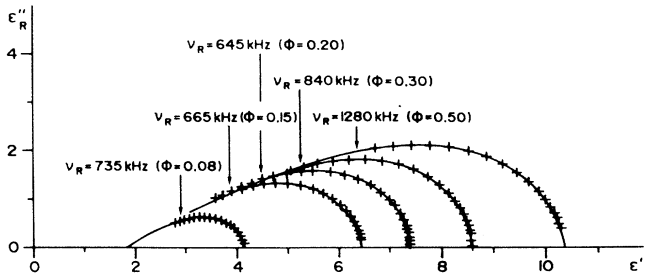


FIG. 16. Formamide-AOT-isooctane system. $T$=25°C; $n$=[formamide]/[AOT]=1.7. Variations of $\epsilon_R''$ vs $\epsilon'$ for $\phi$=0.08, 0.15, 0.20, 0.30, and 0.50.

It will be noted that Eqs. (3) and (5) indicate that the derivative $(1/\sigma)(d\sigma/d\phi)$ tends towards infinity at the percolation threshold.

It should also be observed that Eqs. (2)–(5) are only valid if $|z| \ll 1$. For conductivity this implies that $\sigma_2/\sigma_1 \ll (\phi-\phi_c)^{(\mu+s)}$. They are not valid in the neighborhood of $\phi_c$ in which $|z| \to \infty$. In fact, experimentally, there is a continuous transition within an interval of width $\Delta$ in the immediate neighborhood of $\phi_c$. The width of this transition interval (the crossover regime) is of the order [9] of $\Delta = \delta_1+\delta_2 = (\sigma_2/\sigma_1)^{1/(\mu+s)}$.

Rather than developing $f(z)$ to the first order one can go further and develop $f(z)$ in Eq. (1) to the second order. It can easily be verified [10,11] that the equations predict the existence of dielectric relaxation corresponding to Debye's well-known relationship. Following a suggestion made by Bergman and reported in the literature [11], when $\phi$ is close to $\phi_c$ one can expect the characteristic frequency of the dielectric relaxation to be such that

$$\nu_R \propto |\phi-\phi_c|^{(\mu+s)} , \tag{6}$$

in other words that $\nu_R \to 0$ if $\phi \to \phi_c$.

As regards the dynamic viscosity $\eta$, by analogy with

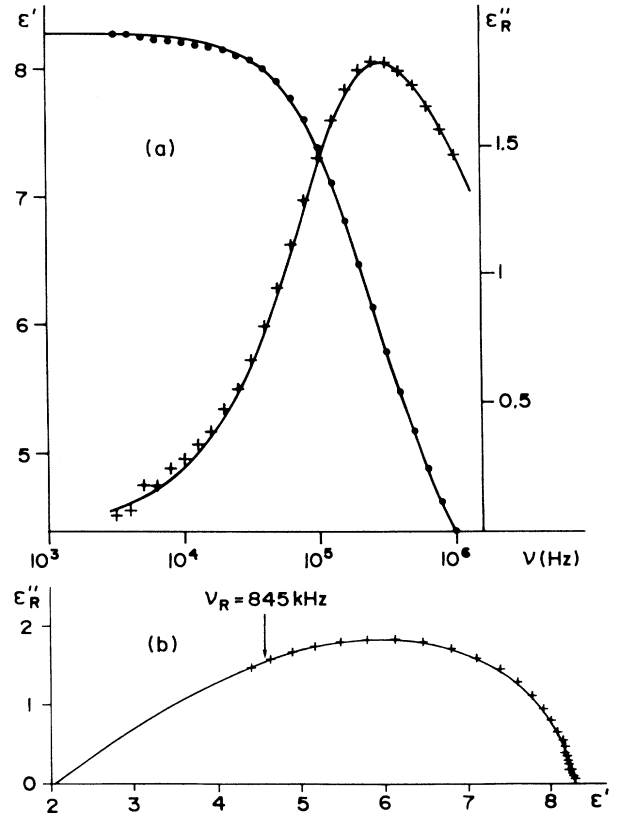


FIG. 17. Formamide-AOT-cyclohexane system. $T$=25°C; $n$=[formamide]/[AOT]=2.5; $\phi$=0.15. (a) Variations of $\epsilon'$ and $\epsilon_R''$ vs frequency. (b) Variations of $\epsilon_R''$ vs $\epsilon'$.

the previous equations the following relations were proposed and verified [2,12]:

$$\eta \propto \begin{cases} \eta_1(\phi-\phi_c)^{\mu'} & \text{if } \phi > \phi_c + \delta_1' \quad (7) \\ \eta_2(\phi_c-\phi)^{-s'} & \text{if } \phi < \phi_c - \delta_2' \, . \quad (8) \end{cases}$$

The transition interval is characterized by $\Delta' = \delta_1' + \delta_2' = (\eta_2/\eta_1)^{1/(\mu'+s')}$. The previous equations predict an increase in $\eta$ with $\phi$, and at the threshold one should theoretically obtain $(1/\eta)(d\eta/d\phi) \rightarrow \infty$.

So experimentally, given the existence of the intervals $\Delta$ and $\Delta'$, the following results can be expected: on the one hand, an increase of $\sigma$ with $\phi$ and movement of $(1/\sigma)(d\sigma/d\phi)$ through a maximum at the threshold. In some cases, as we have mentioned in our discussion, $\epsilon_s(\phi)$ presents a more or less clearly marked maximum at the threshold (in certain cases there may in fact be no maximum at all). At the same time the characteristic frequency $\nu_R$ must go through a minimum. Finally the dynamic viscosity must increase and $(1/\eta)(d\eta/d\phi)$ must go through a maximum at the threshold. Quantitative analysis of the results is only possible if the transition interval ($\Delta$ for conductivity and $\Delta'$ for viscosity) is narrow. A very good fit is obtained between experimental and theoretical values for the conductivity of water-AOT-undecane systems with $\mu = 1.94$ and $s = 1.2$, which clearly reflects the dynamic aspect of the phenomenon [13,14]. Similarly, a quantitative study [2] carried out on waterless glycerol-AOT-isooctane microemulsions gives the following results for dynamic viscosity: $\mu' = 2.00 \pm 0.25$

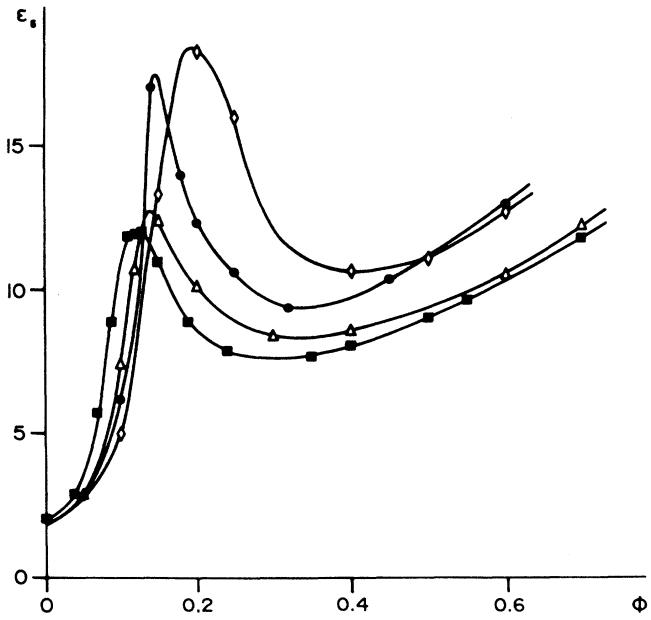


FIG. 18. Glycerol-AOT-isooctane system. $n$=[glycerol]/[AOT]=4. Variations of $\epsilon_s$ vs $\phi$ for different values of $T$: ◇, 10°C; ●, 15°C; △, 20°C; ■, 25°C.

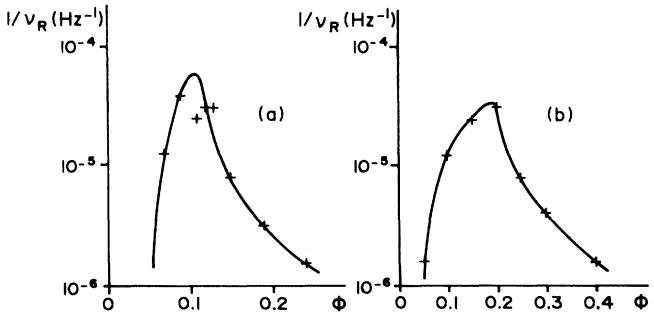


FIG. 19. Glycerol-AOT-isooctane system. $n$=[glycerol]/[AOT]=4. Variations of $1/\nu_R$ vs $\phi$. (a) $T$=25°C,] (b) $T$=10°C.

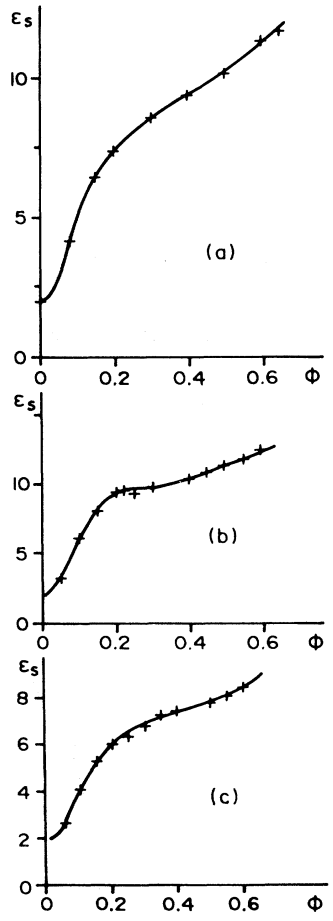


FIG. 20. Variations of $\epsilon_s$ vs $\phi$. (a) Formamide-AOT-isooctane system. $T$=25°C; $n$=[formamide]/[AOT]=1.7. (b) Formamide-AOT-cyclohexane system. $T$=25°C; $n$=[formamide]/[AOT]=2.5. (c) Ethylene glycol-AOT-isooctane system. $T$=25°C; $n$=[ethylene glycol]/[AOT]=2.

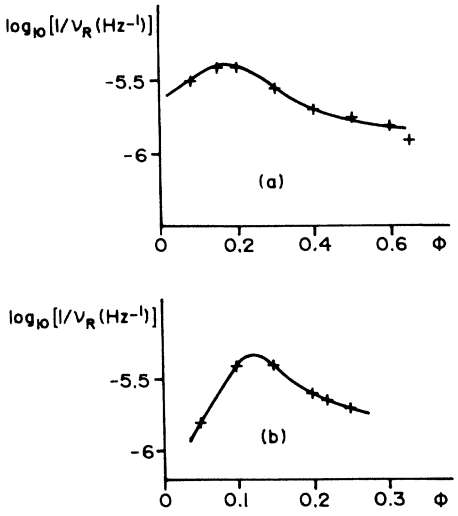


FIG. 21. Variations of $1/\nu_R$ vs $\phi$. (a) Formamide-AOT-isooctane system. $T=25°C$; $n=$[formamide]/[AOT]$=1.7$. (b) Formamide-AOT-cyclohexane system. $T=25°C$; $n=$[formamide]/[AOT]$=2.5$.

and $s'=1.2\pm0.2$, which are practically identical to the figures obtained for conductivity.

## IV. EXPERIMENTAL RESULTS

### A. Water-based ternary microemulsions

We studied several water-AOT-oil-type systems in which the oil was cyclohexane, isooctane, undecane, and dodecane. It is well known for water-AOT-oil systems that at low and intermediate water content values the microemulsion consists of water globules in oil subjected to Brownian motion. For example, for the water-AOT-decane system, neutron-scattering diffusion measurements [15] indicate that there are spherical globules until high values of $\phi$ are reached ($\phi>0.6$). Moreover, for these systems the globules present attractive interactions [16].

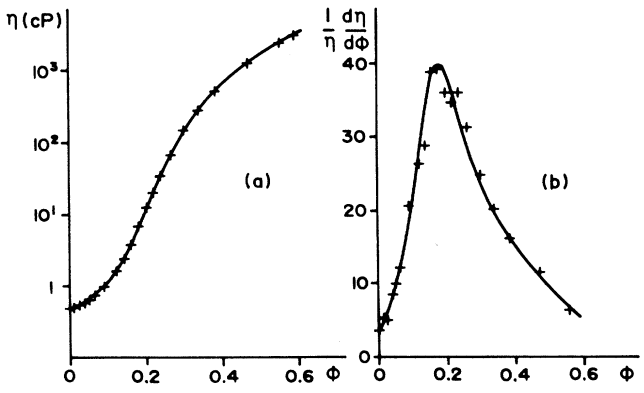


FIG. 22. Glycerol-AOT-isooctane system. $T=25°C$; $n=$[glycerol/AOT]$=2.5$. (a) Variations of $\eta$ vs $\phi$. (b) Variations of $(1/\eta)(d\eta/d\phi)$ vs $\phi$.

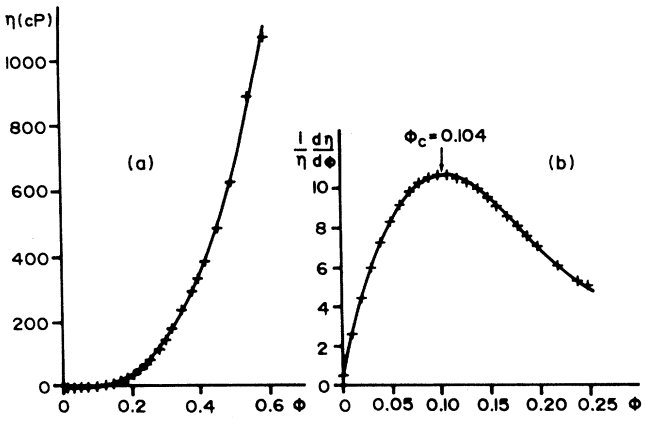


FIG. 23. Formamide-AOT-cyclohexane system. $T=25°C$; $n=$[formamide]/[AOT]$=2.5$. (a) Variations of $\eta$ vs $\phi$. (b) Variations of $(1/\eta)(d\eta/d\phi)$ vs $\phi$.

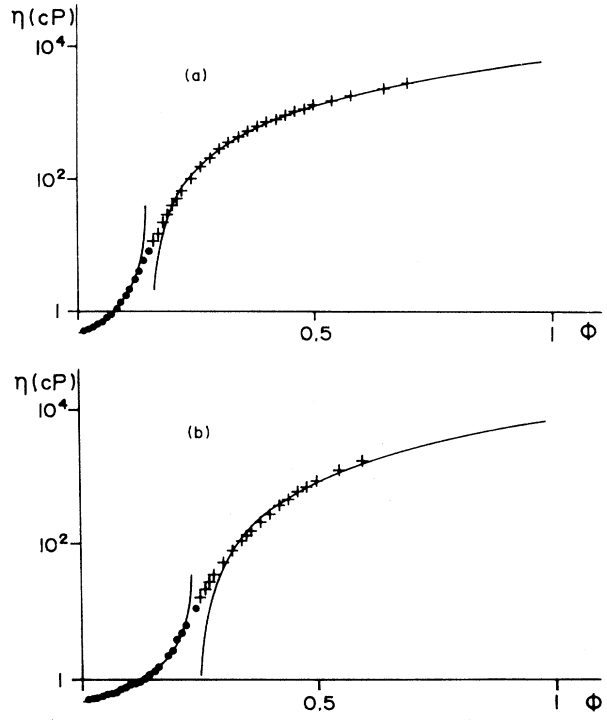


FIG. 24. Glycerol-AOT-isooctane system. Curves $\eta=f(\phi)$. (a) $n=$[glycerol/AOT]$=3.2$. $T=25°C$. (b) $n=$[glycerol]/[AOT]$=2$. $T=25°C$. ——, theoretical curves [Eqs. (7) and (8)].

Figures 1 and 2 represent conductivity for the water-AOT-undecane and water-AOT-dodecane systems. A very rapid increase of $\sigma$ with $\phi$ is observed, whatever the value of the molar ratio $n$=[water]/[AOT]. As the $\sigma_{oil}/\sigma_{water}$ ratio is much lower than unity (oil is practically an insulator), the transition interval is very small and quantitative analysis becomes possible. It can be verified that the associated exponents are 1.94 and $-1.2$, as shown in Fig. 3 representing $\sigma^{-1/1.2}$ ($\phi<\phi_c$) and $\sigma^{1/1.94}$ ($\phi>\phi_c$) as a function of $\phi$ (values normalized at 1 for $\phi=0$ and 1). On Fig. 4 it can be verified that $(1/\sigma)(d\sigma/d\phi)$ does indeed go through a maximum at the threshold.

Figure 5 is an example of the variations of dielectric relaxation $\epsilon_R^*=\epsilon'-j\epsilon_R''$ versus frequency. The Cole-Cole diagram $\epsilon_R''(\epsilon')$ is also represented. It will be observed that there is a Cole-Cole-type distribution characterized by the characteristic frequency $\nu_R$. Figures 6 and 7 correspond to variations of the static permittivity $\epsilon_s$ and the characteristic frequency $\nu_R$ as a function of $\phi$ for the water-AOT-dodecane system. As predicted by the theory, a maximum of $\epsilon_s$ occurs at the same point as a minimum of $\nu_R$.

Finally Figs. 8 and 9 represent variations of the dynamic viscosity $\eta$ as a function of $\phi$ for two different oils. There is a clear increase in $\eta$ when $\phi$ increases. It is not possible to carry out a quantitative analysis on the basis of Eqs. (7) and (8) because the $(\eta_{oil}/\eta_{water})$ ratio is not sufficiently small as regards unity and therefore the transition interval $\Delta'$ is too large. However, qualitatively, apart from the increase of $\eta$ with $\phi$, it is observed that the quantity $(1/\eta)(d\eta/d\phi)$ moves through a maximum (in the neighborhood of the threshold determined by the study of conductivity [12]), as shown in Fig. 10, which represents a satisfactory result.

### B. Waterless ternary microemulsions

In these systems the water is replaced by glycerol, formamide, or ethylene glycol. We studied [17] the following systems: glycerol-AOT-isooctane, formamide-AOT-isooctane, formamide-AOT-cyclohexane, and ethylene

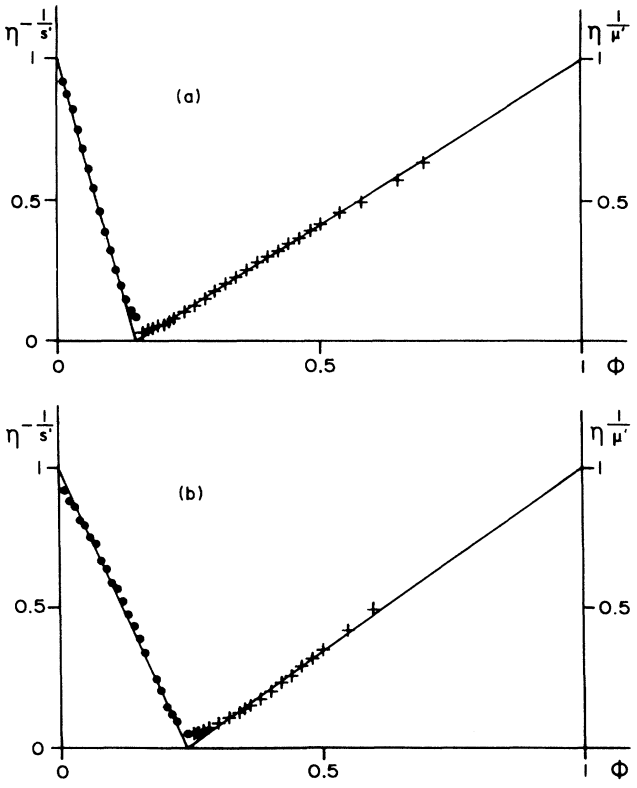


FIG. 25. Glycerol-AOT-isooctane system. Variations of $\eta^{1/\mu'}$ and $\eta^{-1/s'}$ vs $\phi$ (normalized to 1 for $\phi=0$ and 1). ●, $\phi<\phi_c$; +, $\phi>\phi_c$: ——, theoretical curves [Eqs. (7) and (8)]. (a) $n$=[glycerol/AOT]=3.2. $T$=25°C. (b) $n$=[glycerol/AOT]=2. $T$=25°C.

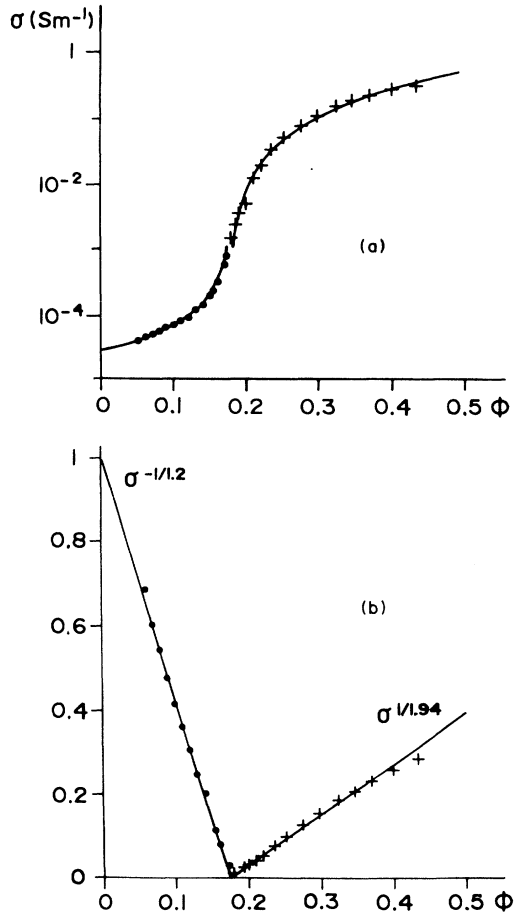


FIG. 26. Water-SDS-butanol-toluene system. $T$=20°C. Initial ratio SDS:butanol=1:2. ——, theoretical curves [Eqs. (3) and (5)]. ●, $\phi<\phi_c$; +, $\phi>\phi_c$. (a) Variations of $\sigma$ vs $\phi$. (b) Variations of $\sigma^{1/\mu}$ and $\sigma^{-1/s}$ vs $\phi$ (normalized to 1 for $\phi=0$ and 1).

glycol-AOT-isooctane. It is reasonable to consider that for these systems in which AOT is the surfactant, the situation is always one of spheres dispersed in a continuous medium. For the similar glycerol-AOT-heptane system studied [18] by neutron-scattering diffusion one obtains spherical glycerol droplets stabilized by the surfactant.

Figure 11 represents variations of conductivity $\sigma$ versus volume fraction $\phi$ for the glycerol-AOT-isooctane system. Figure 12 represents the associated variations of $(1/\sigma)(d\sigma/d\phi)$. This curve presents a maximum. This is also true for the formamide-AOT-cyclohexane system (Fig. 13). Of course it is difficult to carry out a quantitative analysis because in this case the $\sigma_{\text{oil}}/\sigma_{\text{glycerol}}$ (or $\sigma_{\text{oil}}/\sigma_{\text{formamide}}$) ratio is too large and therefore the transition interval $\Delta$ is wide.

Figure 14 displays the variations of dielectric relaxation for the glycerol-AOT-isooctane system. Figure 15 corresponds to the associated $\epsilon_R''(\epsilon')$ diagrams. This yields [10,11,17] a distribution of dielectric relaxation times of the Havriliak-Negami type [19] as a result of the presence of glycerol. This also occurs when the glycerol is replaced by formamide, as shown in Figs. 16 and 17. The curve of variation of static permittivity $\epsilon_s$ vs $\phi$ may assume diverse shapes. Thus, with glycerol, when $\phi$ increases, $\epsilon_s$ moves through a maximum followed by a minimum (Fig. 18) and the associated characteristic frequency $\nu_R$ moves through a minimum (Fig. 19); in other words, the associated characteristic time $1/\nu_R$ goes through a maximum. On the other hand, with formamide and ethylene glycol there are no longer any maxima (Fig. 20): $\epsilon_s$ continues to increase and simply presents an accident on the curve. However, it will be observed that the characteristic frequency moves through a minimum as predicted by Eq. (6) (Fig. 21). As we have already indicated in our theoretical introduction these diverse forms of the function $\epsilon_s(\phi)$ may be interpreted qualitatively, within the framework of percolation theory, by the fact that in Eq. (4) there is competition, when $\phi$ increases, between one increasing term and another decreasing term.

For these waterless ternary systems one can quantitatively analyze the dynamic viscosity $\eta$ when glycerol is present. This is because $\eta_{\text{glycerol}} \gg \eta_{\text{oil}}$ (with isooctane as oil, $\eta_{\text{oil}}/\eta_{\text{glycerol}} = 5\times10^{-4}$ at 25° C and $10^{-4}$ at 10° C). $\Delta'$ is therefore low. Figure 22 represents the $\eta$ and $(1/\eta)(d\eta/d\phi)$ curves as a function of $\phi$ for the glycerol-AOT-isooctane system. Figure 23 corresponds to the formamide-AOT-cyclohexane system. In both examples $\eta$ increases rapidly with $\phi$ and $(1/\eta)(d\eta/d\phi)$ moves through a maximum. Using relationships (7) and (8) numerical analysis becomes possible. Figures 24 and 25 il-

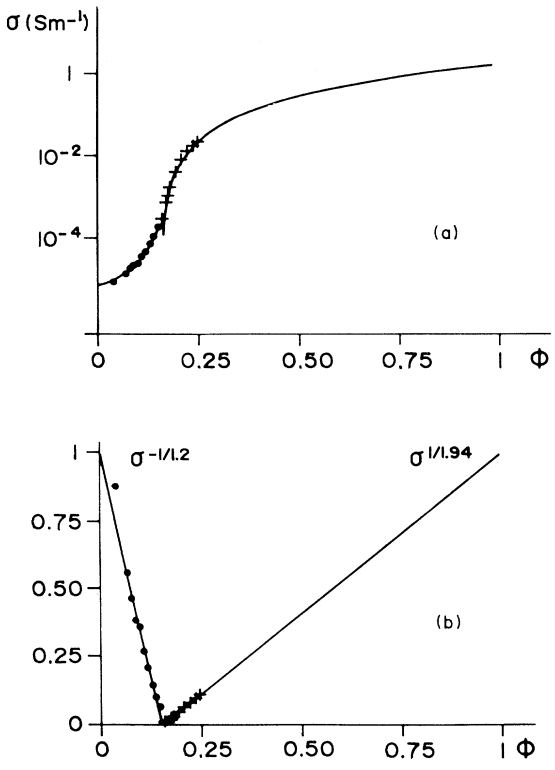


FIG. 27. Water-SDS-butanol-toluene system. $T=20$°C. Initial ratio SDS:butanol=1:3. ——, theoretical curves [Eqs. (3) and (5)]. ●, $\phi<\phi_c$; +, $\phi>\phi_c$. (a) Variations of $\sigma$ vs $\phi$. (b) Variations of $\sigma^{1/\mu}$ and $\sigma^{-1/s}$ vs $\phi$ (normalized to 1 for $\phi=0$ and 1).

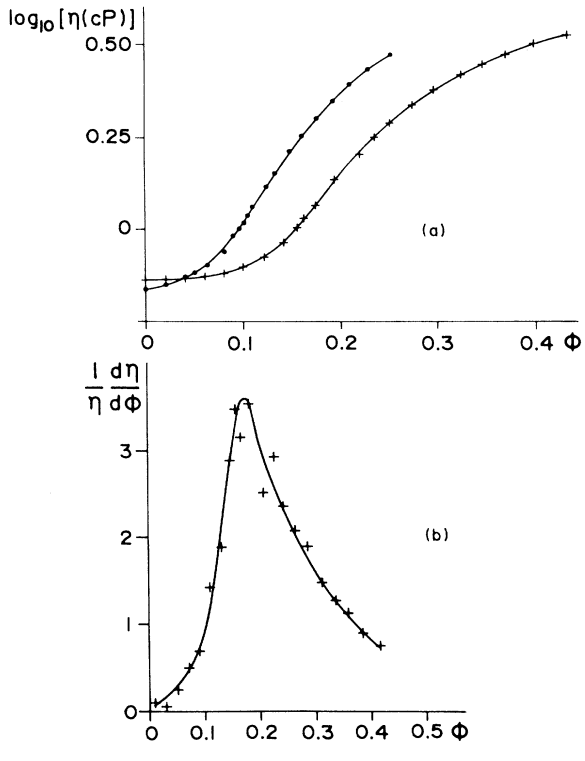


FIG. 28. Water-SDS-butanol-toluene system. $T=20$°C. (a) Variations of $\log_{10}(\eta)$ vs $\phi$. +, initial ratio SDS:butanol=1:2. ●, initial ratio SDS:butanol=1:3. (b) Variations of $(1/\eta)(d\eta/d\phi)$ vs $\phi$. Initial ratio SDS:butanol=1:2.

lustrate the excellent fit obtained between experimental and theoretical curves by taking $\mu' \approx 2$ and $s' \approx 1.2$.

### C. Quaternary water-SDS-butanol-toluene systems

As all the above systems were ternary we believed it would be interesting to undertake the study of a quaternary system, the water-SDS-butanol-toluene system (SDS is sodium dodecyl sulfate). The alcohol is distributed between the continuous and interfacial phases, and as analysis of the results requires knowledge of the volume fraction $\phi$ in dispersed matter (water+interfacial phase) one needs to be careful in choosing the samples to study.

This system has already been the object of a good deal of research [20,21], and it corresponds to the model of spheres dispersed in a continuous medium. The surfactant SDS is insoluble in the toluene and butanol. It is entirely located in the dispersed phase. The continuous phase is a mixture of toluene, butanol, and water. In these circumstances, assuming that all the water in the mixture is in the micelles would lead to an error in the determination of $\phi$. Compared with ternary microemulsions for which it is enough to simply mix in some oil, the dilution of quaternary microemulsions is much more complex. For the system studied here the butanol is soluble in the toluene and can also dissolve as much as 20% water. The interfacial layer contains some of the alcohol, some of the toluene, and all the SDS. The interior of the micelle is made up of practically pure water (the solubility of butanol in water is extremely low).

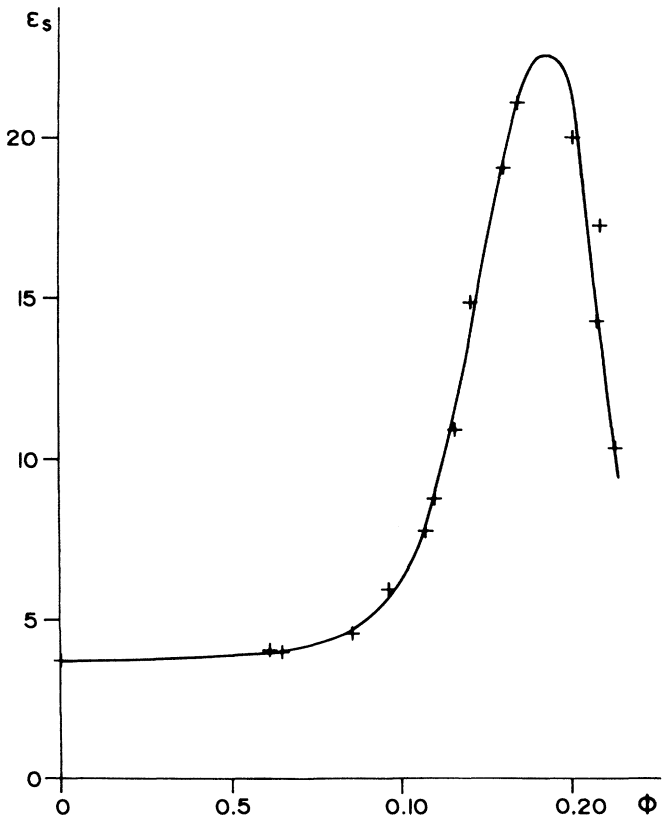


FIG. 29. Water-SDS-butanol-toluene. $T=20°C$. Initial ratio SDS:butanol=1:2. Variations of $\epsilon_s$ vs $\phi$.

Using the dilution method and data indicated in the literature [20,21] it is possible with this system to achieve a conservating dilution, in other words, one which maintains the composition and dimension of the micelles constant. During dilution the SDS:butanol ratio is not constant and the figurative point of the microemulsion is displaced along the demixtion surface in the phase diagram, and does not remain in a pseudoternary plane. The method implies that investigation should be restricted to systems which are initially located on the demixtion line of the ternary pseudo-diagram associated with the initial SDS:butanol ratio. For these systems, the composition of the different phases can be determined, and thus throughout dilution $\phi$ is perfectly clearly identified.

Figures 26 and 27 represent variations of conductivity for two microemulsions initially located on the demixtion line of the pseudoternary planes SDS:butanol=1:2 and 1:3. It can be observed that there is an excellent fit between experimental and theoretical results and that the percolation exponents still have the values 1.94 and $-1.2$. Figure 28 represents variations of dynamic viscosity. It is not possible to carry out quantitative analysis because the transition internal $\Delta'$ is too wide. However, it can be seen that $\eta$ increases with $\phi$ and that $(1/\eta)(d\eta/d\phi)$ moves through a maximum for an identical value at the percolation threshold determined by conductivity. The same also holds for the dielectric constant $\epsilon_s$ as shown in Fig. 29.

## V. CONCLUSION

All these systems correspond to a dispersion of spheres in a continuous medium, the spheres undergoing Brownian motion. The dynamic description of the phenomenon of percolation applies and, qualitatively, the theoretical predictions are verified: increase in the conductivity $\sigma$ and the dynamic viscosity $\eta$ with the dispersed matter content $\phi$, the almost simultaneous passage of $(1/\sigma)(d\sigma/d\phi)$, $(1/\eta)(d\eta/d\phi)$, $1/\nu_R$, and possibly also $\epsilon_s$ through a maximum at the percolation threshold. Quantitatively, it is very satisfying to observe that when the conditions of application of the asymptotic laws of the theory are satisfied the scale exponents are the same, in other words $\simeq 2$ above the threshold and $\simeq -1.2$ below the threshold, whatever the property studied and whatever the chemical nature of the components, irrespective of whether the system is ternary or quaternary. This indicates that all these systems belong to the same class of universality.

It should be pointed out as a concluding remark that within the model of spheres in a continuous medium, it was possible to calculate the shape of the percolation threshold line in the $\phi$-$T$ plane [17,22,23] by using models recently introduced for simple fluids [24]. A very good fit was obtained both for the water-AOT-decane ternary system [22] and for the glycerol-AOT-isooctane ternary sys-

tem [17,23]. This corresponds once again to the generality of the description of the behavior of these systems, in terms of the class of universality of dynamic systems of spheres in a continuum.

ACKNOWLEDGMENT

The Laboratoire de Physique des Matériaux Industriels is "Unité de Recherche associée au CNRS no. 1494."

[1] M. Lagues, R. Ober, and C. Taupin, J. Phys. Lett. (Paris) **39**, L487 (1978).
[2] Z. Saidi, C. Mathew, J. Peyrelasse, and C. Boned, Phys. Rev. A **42**, 872 (1990).
[3] C. Boned and J. Peyrelasse, J. Surf. Sci. Tech. **71**, 1 (1991).
[4] M. A. Van Dijk, Phys. Rev. Lett. **55**, 1003 (1985).
[5] S. Bhattacharya, J. P. Stokes, M. W. Kim, and J. S. Huang, Phys. Rev. Lett. **55**, 1884 (1985).
[6] J. Peyrelasse, M. Moha-Ouchane, and C. Boned, Phys. Rev. A. **38**, 904 (1988).
[7] C. Cametti, P. Codastefano, A. Di Biasio, P. Tartaglia, and S. H. Chen, Phys. Rev. A **40**, 1962 (1989).
[8] C. Cametti, P. Codastefano, P. Tartaglia, S. H. Chen, and J. Rouch, Phys. Rev. A **45**, R5358 (1992).
[9] A. L. Efros and B. L. Shklovskii, Phys. Status Solidi B **76**, 475 (1976).
[10] C. Mathew, Z. Saidi, J. Peyrelasse, and C. Boned, Phys. Rev. A **43**, 873 (1991).
[11] L. Benguigui, J. Yacubovicz, and M. Narkis, J. Polym. Sci. B **25**, 127 (1987).
[12] J. Peyrelasse, M. Moha-Ouchane, and C. Boned, Phys. Rev. A **38**, 4155 (1988).
[13] M. Lagues, J. Phys. Lett. (Paris) **40**, 6331 (1979).
[14] G. S. Grest, J. Webman, S. A. Safran, and A. L. R. Bug, Phys. Rev. A **33**, 2842 (1986).
[15] M. Kotlarchyk, S. H. Chen, J. S. Huang, and M. W. Kim, Phys. Rev. Lett. **53**, 941 (1984).
[16] J. S. Huang, S. A. Safran, M. W. Kim, G. S. Grest, M. Kotlarchyk, and N. Quirke, Phys. Rev. Lett. **53**, 592 (1984).
[17] Z. Saidi, Thèse de Doctorat, Université de Pau, France, 1991.
[18] P. D. I. Fletcher, M. F. Galal, and B. H. Robinson, J. Chem. Soc. Faraday Trans. 1 **80**, 3307 (1984).
[19] S. Havriliak and S. Negami, J. Polymer Sci. C. **14**, 99 (1966).
[20] A. Graciaa, Thèse de Doctorat, Université de Pau, France, 1978.
[21] A. Graciaa, J. Lachaise, A. Martinez, M. Bourrel, and C. Chambu, C.R. Acad. Sci. Paris, **282B**, 547 (1976).
[22] C. Cametti, P. Codastefano, P. Tartaglia, J. Rouch, and S. H. Chen, Phys. Rev. Lett. **64**, 1461 (1990).
[23] Z. Saidi, C. Boned, and J. Peyrelasse, Prog. Colloid Polym. Sci. **89**, 156 (1992).
[24] J. Xu and G. Stell, J. Chem. Phys. **89**, 1101 (1988).